





Nonacoustic high-frequency collective excitations in a ZrCuAl metallic glassTaras Bryk ^{1,2} Noël Jakse ³ Giancarlo Ruocco ^{4,5} and Jean-François Wax ⁶¹*Institute for Condensed Matter Physics, National Academy of Sciences of Ukraine, UA-79011 Lviv, Ukraine*²*Institute of Applied Mathematics and Fundamental Sciences, Lviv National Polytechnic University, UA-79013 Lviv, Ukraine*³*Université Grenoble Alpes, CNRS, Grenoble INP, SIMaP, F-38000 Grenoble, France*⁴*Center for Life Nano Science @Sapienza, Istituto Italiano di Tecnologia, 295 Viale Regina Elena, I-00161 Roma, Italy*⁵*Dipartimento di Fisica, Università di Roma “La Sapienza,” I-00185 Roma, Italy*⁶*LCP-A2MC, Université de Lorraine, Metz, 57000, France*

(Received 4 April 2022; revised 30 September 2022; accepted 28 October 2022; published 10 November 2022)

We report a combined theoretical and simulation study of collective excitations in the three-component metallic glass $\text{Zr}_{46}\text{Cu}_{46}\text{Al}_8$. It is shown in that case how one can combine partial current time correlation functions to represent them via total mass and mass-concentration currents, which for the long-wavelength region separately describe hydrodynamic acoustic and nonhydrodynamic opticlike modes. We present dispersions of the longitudinal and transverse acoustic and optic modes over a wide range of wave numbers. Our theoretical analysis of dispersion and damping of three transverse short-wavelength modes sets the basis for the interpretation of already existing experimental data, where the presence of three modes has been disregarded leading to an overestimation of the alleged transverse mode damping.

DOI: [10.1103/PhysRevB.106.174203](https://doi.org/10.1103/PhysRevB.106.174203)**I. INTRODUCTION**

Collective excitations in disordered systems such as liquids and glasses have many specific features not observed in crystalline solids [1]. For the case of liquids the long-wavelength acoustic modes are governed by macroscopic conservation laws, which results in the hydrodynamic mechanism of propagation of longitudinal sound and the absence of transverse sound excitations in the long-wavelength region of the spectrum [2,3]. For glasses the very specific features of collective dynamics are the emergence of nonergodicity upon glass transition and a boson peak feature in the vibrational density of states. Hence very different theoretical approaches are needed to predict theoretically dispersion of collective excitations in the liquid and glassy states, although there are attempts to suggest a unified approach [4] that causes corresponding criticism [5]. Theoretical description of excitations in glasses within the harmonic approximation [6–8], the recently suggested projection formalism accounting for retardation and nonlocality in sound propagation [9], and estimation of the role of Ioffe-Regel crossover in dynamics [10,11] form the basis for the actual understanding of acoustic excitations in glasses.

Collective dynamics in multicomponent disordered systems is essentially different from the case of pure ones. Collective excitations are not limited only to the usual acoustic longitudinal and transverse propagating modes as in the one-component case, but contain also damped opticlike excitations. For binary glasses, in contrast to liquids, the opticlike collective modes are well defined and were studied by molecular dynamics (MD) simulations [12,13] and by inelastic neutron scattering [14]. For the case of multi-component glasses with three and more species, discussion about possible

opticlike excitations observed either in simulation or in experimental studies is very rare. In Ref. [15] the authors simulated the dynamics of binary $\text{Pd}_{82}\text{Si}_{18}$ and ternary $\text{Zr}_{50}\text{Cu}_{40}\text{Al}_{10}$ metallic glasses in order to obtain the dispersion of acoustic longitudinal and transverse excitations. They studied the frequency spectra of wave-number-dependent total current autocorrelation functions, while partial quantities (such as partial dynamic structure factors) were used only to highlight the dynamics of the lightest component of the binary and ternary glass. There are many experimental and simulation papers on the structure, relaxation dynamics, and transport properties of multi-component glasses [16–23]; however, the existence of optic modes and their effect on dynamics were not discussed.

For the case of binary and multi-component liquids the situation with experimental observation of opticlike modes [24] is worse because of their essentially stronger damping in liquids than in glasses. In general, for liquids, optic modes belong to nonhydrodynamic processes [25], i.e., are not connected to fluctuations of conserved quantities, and therefore it is impossible to observe the most long-wavelength optic modes in scattering experiments, while a small overdamped signal can be extracted from the experimental dynamic structure factor outside the hydrodynamic region [26,27]. In contrast to the scattering experiments in MD simulations the presence of opticlike modes is clearly manifested in the shape of mass-concentration current autocorrelation functions [28,29]. Among the numerous classical and *ab initio* simulation studies of binary liquids which one can find in the literature, some were simulation studies of dynamics in three-component liquids or glasses [15,30,31]; however, practically, there were no reports on theoretical analysis of collective excitations in three-component disordered

systems and their dispersions and dampings except in Refs. [32–35].

Very recently [35], in inelastic neutron scattering experiments on a ternary metallic glass, $\text{Zr}_{46}\text{Cu}_{46}\text{Al}_8$, the authors reported an unexpected feature for transverse excitations in this multi-component glass. Specifically, they observed that the damping of the transverse phonon modes plotted as a function of wave number mirrors the shape of the static structure factor $S(k)$. The authors' interpretation is about the existence of a universal correlation between the transverse phonon dynamics and the underlying disordered structure. There is, however, an inherent difficulty in separating, in the experimental scattering intensity, different contributions from longitudinal acoustic (LA) and optic (LO) as well as transverse acoustic (TA) and optic (TO) modes, which was not discussed. On the other hand, in computer simulation the optic modes, although overdamped, are well defined in binary and multicomponent glasses [12,13]. Apparently, from the experiments, no optical mode could be seen in $\text{Zr}_{46}\text{Cu}_{46}\text{Al}_8$ experimental spectra, which are rather dominated by the acoustic modes [35]. These controversial results prompt us to perform a deeper analysis of transverse and longitudinal excitation in multi-component glasses.

The aim of the present work is to perform MD simulations of $\text{Zr}_{46}\text{Cu}_{46}\text{Al}_8$ glass with the same embedded-atom model (EAM) potentials [35] in order to check the spectra of LA, LO, TA, and TO collective excitations; separate contributions from optic modes to the time-dependent correlations; and, via that methodology, check the finding of Ref. [35] concerning the k dependence of damping for transverse acoustic modes. The remaining paper is organized as follows: In the next section we will provide details of simulations for the $\text{Zr}_{46}\text{Cu}_{46}\text{Al}_8$ metallic glass and corresponding analysis of collective excitations in the three-component system. In Sec. III we report our results for static structure, analysis of the time-dependent correlations, dispersions of collective excitations, and wave number dependence of damping of transverse acoustic modes. Section IV will present the conclusions of this study.

II. SIMULATIONS AND DETAILS OF ANALYSIS

We performed molecular dynamics simulations for the $\text{Zr}_{46}\text{Cu}_{46}\text{Al}_8$ metallic glass in the isobaric-isothermal (NPT) and isochoric-isothermal (NVT) ensembles using the Large-Scale Atomic/Molecular Massively Parallel Simulator (LAMMPS) code [36]. The interatomic interactions were represented by the EAM potentials [37]; using two system sizes, namely, $N = 2000$ and $N = 11\,664$ atoms, we checked that the smaller system did not display size effects and was sufficient for sampling of various partial dynamic variables of density, mass currents, components of the stress tensor, etc., with different directions of \mathbf{k} vectors along the phase-space trajectory. The atoms of different species were placed randomly on a grid in a cubic simulation box of volume V subject to the standard periodic boundary conditions (PBCs). The initial configuration of atoms was kept for 100 ps at $T = 2000$ K in order to obtain the equilibrated liquid phase. The equations of motion are solved using Verlet's algorithm in the velocity form with a time step of 1 fs. Quenching at zero pressure from the melt at 2000 K to 300 K was

carried out at a cooling rate of 10^{11} K/s. Such a cooling rate was shown to be appropriate for the glass formation for this type of alloy [38–40], with negligible influence of the history of the cooling. The final equilibration in the (NPT) ensemble resulted in average atomic density of the glass $n = N/V = 0.0574 \text{ \AA}^{-3}$. Using this density, the simulation was subsequently continued for the production of the phase-space trajectory in the canonical ensemble (NVT) with a Nosé-Hoover thermostat, typically during 200 ps at $T = 300$ K, from which we computed the structural and dynamic properties.

The main idea behind the search for nonacoustic excitations is the separation of contributions from different excitations either to time-dependent correlations or to their Fourier spectra. The simplest methodology was presented for the case of binary systems in Ref. [29] for transverse dynamics and in Ref. [41] for longitudinal dynamics, where a combination of two partial mass currents was able to represent separately the well-defined high-frequency oscillations of the corresponding autocorrelation function due to opticlike excitations. However, the dynamics of a three-component system is much more complex than the case of binary disordered systems. We would need to find three combinations of partial mass currents, which would represent three different oscillation contributions to time-dependent correlations. We start from definitions of longitudinal (L) and transverse (T) partial mass currents

$$J_{\alpha}^{L/T}(k, t) = \frac{m_{\alpha}}{\sqrt{N_{\alpha}}} \sum_{j=1}^{N_{\alpha}} v_{j,\alpha}^{L/T}(t) e^{-i\mathbf{k}\mathbf{r}_{j,\alpha}(t)}, \quad \alpha = \text{Zr, Cu, Al}, \quad (1)$$

where $v_{j,\alpha}^{L/T}(t)$ is the longitudinal or transverse component of the particle velocity and the summation for each partial mass current is performed over the particles of kind α . The total mass current is simply

$$J_{\text{tot}}^{L/T}(k, t) = \sqrt{c_{\text{Zr}}} J_{\text{Zr}}^{L/T}(k, t) + \sqrt{c_{\text{Cu}}} J_{\text{Cu}}^{L/T}(k, t) + \sqrt{c_{\text{Al}}} J_{\text{Al}}^{L/T}(k, t), \quad (2)$$

where $c_{\alpha} = N_{\alpha}/N$ are concentrations. The corresponding mass concentrations are $x_{\alpha} = m_{\alpha}N_{\alpha}/\bar{m}$ and $\bar{m} = m_{\text{Zr}}N_{\text{Zr}} + m_{\text{Cu}}N_{\text{Cu}} + m_{\text{Al}}N_{\text{Al}}$. We would like to stress that there is a difference in “number-concentration” (Bhatia-Thornton) and “total mass–mass-concentration” representations of collective dynamics in many-component systems [42]. Since the conserved quantity is the total momentum of the system, we will proceed further within the total mass–mass-concentration representation. Our task now is to find two more combinations of the partial mass currents, which would be orthogonal to the total mass current; that is, the averaged instantaneous cross correlations are zero:

$$\langle J_{\text{tot}}^{L/T}(k) J_x^{L/T}(-k) \rangle = 0. \quad (3)$$

The standard averages $\langle \dots \rangle$ are over the ensemble of configurations in the NVT ensemble, and for time correlation functions this means the average over the ensemble of functions with different origins too. Since two heavier components (Zr and Cu) are present in the studied glass with equivalent and much higher concentrations than for the third, light component (Al), we will try a mutual mass-concentration current

involving just heavier A and B components:

$$J_{x1}^{L/T}(k, t) = x_{\text{Cu}}\sqrt{c_{\text{Zr}}}J_{\text{Zr}}^{L/T}(k, t) - x_{\text{Zr}}\sqrt{c_{\text{Cu}}}J_{\text{Cu}}^{L/T}(k, t), \quad (4)$$

which describes the motion of two partial mass currents of heavier components with opposite directions. One can make sure that the dynamic variables $J_{\text{tot}}^{L/T}(k, t)$ and $J_{x1}^{L/T}(k, t)$ satisfy condition (3) taking into account the relation

$$\langle J_{\alpha}^{L/T}(k)J_{\beta}^{L/T}(-k) \rangle = m_{\alpha}k_B T \delta_{\alpha\beta}, \quad \alpha, \beta = \text{Zr, Cu, Al},$$

where $\delta_{\alpha\beta}$ is the Kronecker symbol, k_B is the Boltzmann constant, and T is the temperature. The third dynamic variable we can compose from the partial mass currents as a mutual current of two heavier components against the mass current of the light component:

$$J_{x2}^{L/T}(k, t) = x_{\text{Al}}[\sqrt{c_{\text{Zr}}}J_{\text{Zr}}^{L/T}(k, t) + \sqrt{c_{\text{Cu}}}J_{\text{Cu}}^{L/T}(k, t)] - [x_{\text{Zr}} + x_{\text{Cu}}]\sqrt{c_{\text{Al}}}J_{\text{Al}}^{L/T}(k, t), \quad (5)$$

and, again, one can check that this dynamic variable is orthogonal to both $J_{\text{tot}}^{L/T}(k, t)$ and $J_{x1}^{L/T}(k, t)$. Hence we have three mutually orthogonal dynamic variables (2), (4), and (5), which in contrast to partial mass currents describe one total and two mutual mass currents in the system. In the next section we will apply these dynamic variables to analysis of current-current time correlation functions

$$F_{J_{\alpha}J_{\beta}}^{L/T}(k, t) = \langle J_{\alpha}^{L/T}(k, t)J_{\beta}^{L/T}(-k, 0) \rangle \quad (6)$$

and corresponding spectral functions in the studied three-component metallic glass. We define the longitudinal (L) and transverse (T) current spectral functions as follows:

$$C_{J_{\alpha}J_{\beta}}^{L/T}(k, \omega) = \frac{1}{\bar{m}k_B T} \int_0^{\infty} F_{J_{\alpha}J_{\beta}}^{L/T}(k, t) dt. \quad (7)$$

Another method of analysis of collective dynamics in disordered systems is the approach of generalized collective modes (GCMs) [43,44], which has been many times successfully applied analytically and numerically to various liquids for estimation of nonhydrodynamic effects such as ‘‘positive sound dispersion’’ [13], heat waves [45], short-wavelength shear waves [46–49], and opticlike modes in binary liquids [29,41,50]. It works very well for exponentially decaying time correlations in liquids, while for supercooled states and glasses it needs a modification in order to account for slow dynamic processes at supercooling and the emergence of non-ergodicity in the glassy state. These slow dynamic processes cannot be reproduced by the standard GCM scheme based on systematic improvement of short-time behavior (frequency moments) in the description of time correlations due to exact sum rules (extension of the set of dynamic variables by their time derivatives). In Ref. [13] such an extended scheme was proposed for the case of glasses, when additional sum rules for time moments of corresponding time correlation functions were taken into account. The same scheme appeared to be very useful for the case of transverse dynamics of highly compressed metallic liquids [51], when in addition to shear waves another contribution from propagating modes emerged in the transverse current spectral functions outside the first pseudo-Brillouin zone. In the next section we will apply the modification of GCM [51] to estimation of the k -dependent

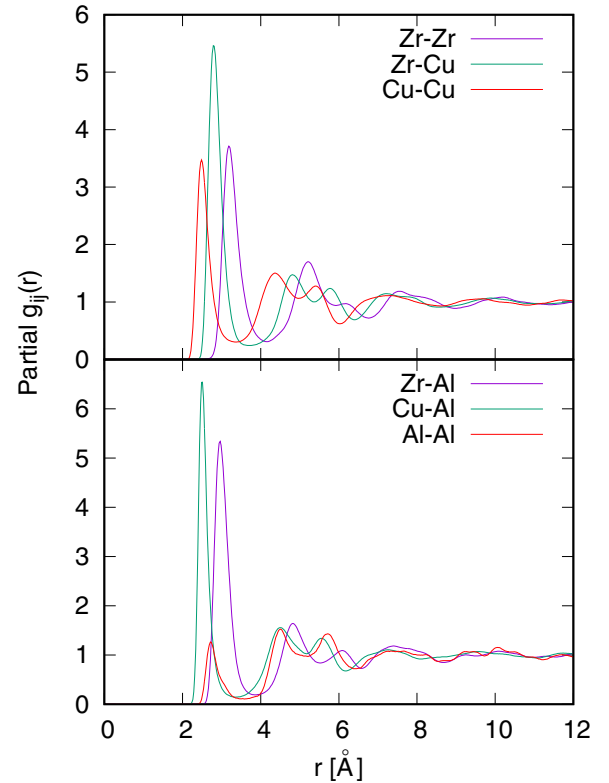


FIG. 1. Partial pair distribution functions for the ternary $\text{Zr}_{46}\text{Cu}_{46}\text{Al}_8$ metallic glass at 300 K.

damping of transverse acoustic modes in the studied three-component glass in order to verify the finding of Ref. [35].

III. RESULTS AND DISCUSSION

A. Static properties and vibrational density of states

We start from the partial pair distribution functions $g_{ij}(r)$ and static structure factor $S(k)$. In Fig. 1 we show six partials, $g_{ij}(r)$, $i, j = \text{Zr, Cu, Al}$, which give evidence that the first coordination shell around Zr or Cu is preferably formed by the other component and the large effective size of Zr atoms plays a role too. Atoms of Al are mostly surrounded by Zr and Cu atoms. The specific-for-glasses splitting of the second maximum of $g_{ij}(r)$ is well observed for all six partial functions.

We are interested in the total static structure factor, defined in the standard way as $S(k) = \langle n_{\text{tot}}(k)n_{\text{tot}}(-k) \rangle$, where $n_{\text{tot}}(k)$ are the spatial-Fourier components of the total number density of particles. However, in order to compare the static structure factor with x-ray experiments [35], we need to use x-ray weighting of partial structure factors because of the different electron densities of Zr, Cu, and Al atoms, hence resulting in the $S_X(k)$ shown in Fig. 2. The main peak of $S_X(k)$ is located at $k_p = 2.71 \text{ \AA}^{-1}$, and $k_p/2$ defines the boundary of the first pseudo-Brillouin zone. The static structure factor obtained from our simulations is in good agreement with the total structure factor of Ref. [35] and especially with the measured first peak position of $k_p = 2.74 \text{ \AA}^{-1}$. The slight shift towards small k of the MD curve might be attributed to a slightly lower density from the NPT simulations.

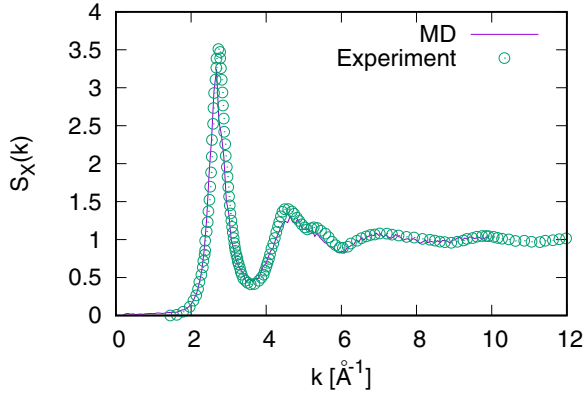


FIG. 2. Structure factor $S_X(k)$ from x-ray diffraction for the ternary $Zr_{46}Cu_{46}Al_8$ metallic glass at 300 K. The MD curve calculated from the Debye formula is compared with the experiment of Ref. [35]. The main peak of the total structure factor is located at $k_p = 2.71 \text{ \AA}^{-1}$, which defines the boundary of the first pseudo-Brillouin zone at $k_p/2$.

From the velocity autocorrelation functions we can estimate the vibrational density of states (VDOS), which will be helpful for analysis of the calculated dispersion curves. The VDOS for the three-component glass was defined as

$$g(\omega) = \frac{\bar{m}}{Nk_B T} \sum_{i=1}^N \int_0^\infty \langle \mathbf{v}_i(t) \mathbf{v}_i(0) \rangle e^{i\omega t} dt, \quad (8)$$

which is practically the same expression as in Ref. [52] but with the dimension of inverse frequency. One can see in Fig. 3 that the main maximum of the VDOS is observed at frequencies of $\sim 16 \text{ ps}^{-1}$, then for higher frequencies of $\sim 20 \text{ ps}^{-1}$ one observes a shoulder, and in the very high frequency region a well-defined smeared peak at $\sim 35\text{--}40 \text{ ps}^{-1}$ is present. Let us calculate the dispersion curves of longitudinal and transverse acoustic and nonacoustic modes in order to clarify the features of the VDOS.

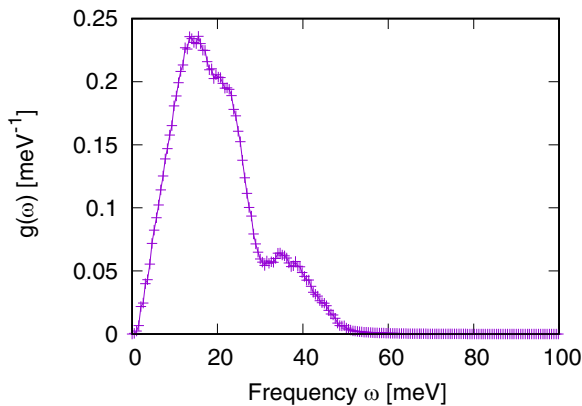


FIG. 3. Vibrational density of states (VDOS) $g(\omega)$ for the ternary $Zr_{46}Cu_{46}Al_8$ metallic glass at 300 K. The VDOS was obtained from velocity autocorrelation functions via Eq. (8).

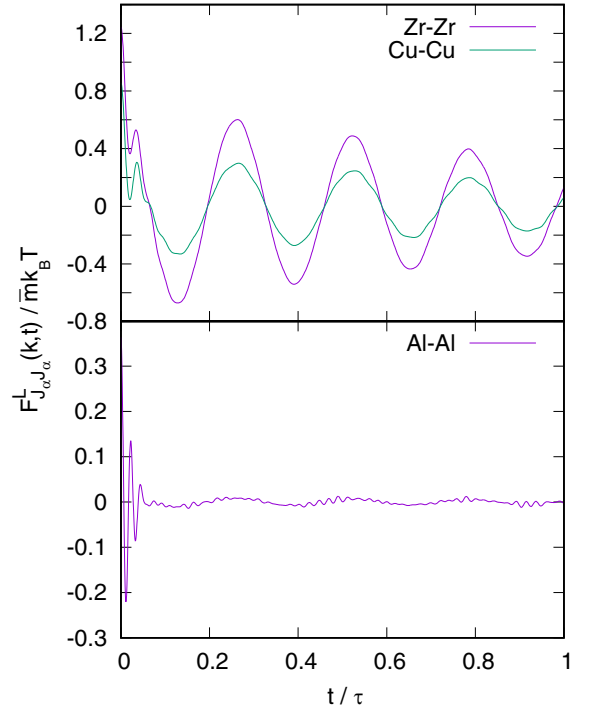


FIG. 4. Longitudinal partial mass-current autocorrelation functions $F_{J_{\alpha}}^L(k, t)$, $\alpha = \text{Zr, Cu, Al}$, at wave number $k = 0.1069 \text{ \AA}^{-1}$. Fast oscillations at short times in the Zr and Cu partial current autocorrelations do not coincide with the frequency of damped oscillations in Al partial current autocorrelations and provide evidence of specific short-time dynamic correlations between two heavier species of the studied ternary glass. The time scale τ is 5.074 16 ps .

B. Current-current time correlation functions in different representations

In order to calculate dispersion curves from current spectral functions in the case of multi-component systems, it is not sufficient to study only total current fluctuations. A very specific feature of collective dynamics in multi-component disordered systems is the intrinsic collective nature of propagating modes, when all the species take part in collective motion, while in the short-wavelength region the dynamics mainly represents single-particle vibrations, and can easily be represented by partial currents (see Ref. [29] for this crossover in the case of transverse dynamics of binary systems). For the three-component glass we show in Fig. 4 how the three partial current-current time correlation functions contain information about different high- and low-frequency excitations.

Using the suggested linear combinations of partial currents (2), (4), and (5), we are able to obtain in the low- k region three current-current time correlation functions, each of which reflects a single damped oscillation (Fig. 5) with very different frequencies. Note that L and T time correlation functions for the combinations (4) and (5) are practically identical, which is absolutely correct when these time correlation functions reflect opticlike excitations in metallic systems, because for metallic systems LO and TO modes do not show a frequency gap at the Γ point.

The current spectral functions corresponding to partial currents and linear combinations (2), (4), and (5) are shown in

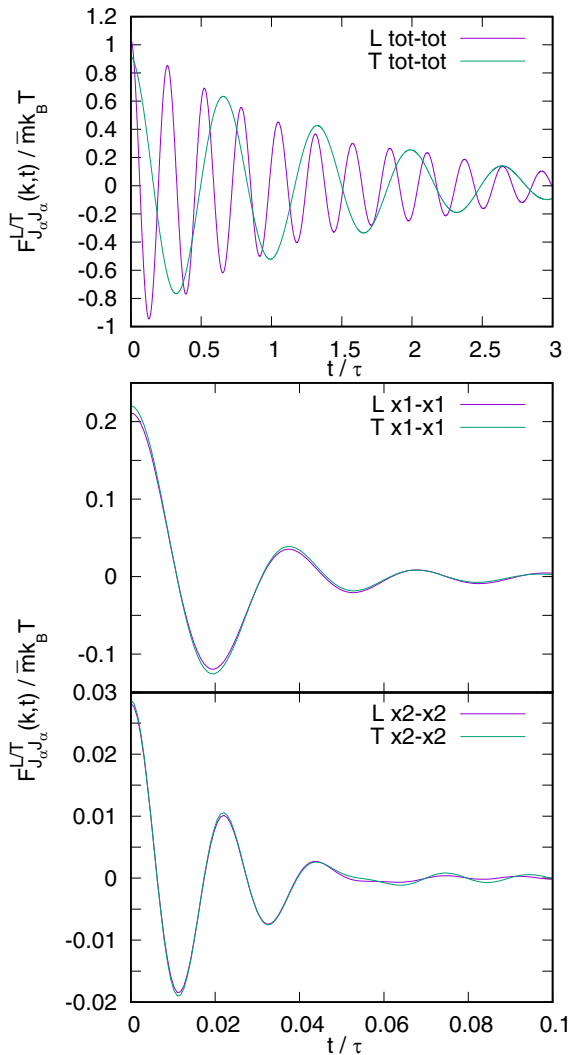


FIG. 5. Longitudinal (purple lines) and transverse (green lines) total mass-current and mass-concentration autocorrelation functions $F_{J_{\alpha}J_{\alpha}}^{L/T}(k,t)$, $\alpha = \text{tot}, x1, x2$, at wave number $k = 0.1069 \text{ \AA}^{-1}$. The long-wavelength total mass-current autocorrelation functions do not contain short-time fast oscillations like the partial mass-current autocorrelation functions in Fig. 4. The time scale τ is 5.074 16 ps.

Fig. 6, and one can see that the partial spectral functions for small wave numbers contain a combination of several smeared peaks, while the current spectral functions of (2), (4), and (5) have just a single-mode contribution. This tendency is general for the long-wavelength region, which allows us to clearly estimate the dispersion of nonacoustic modes.

C. Dispersion of longitudinal and transverse collective modes

Using the peak positions in spectral functions of linear combinations (2), (4), and (5), we easily estimate the dispersion curves of collective excitations, shown in Fig. 7. One should note that the single-peak shape of collective current spectral functions using combinations (2) and (4) gradually changed with increasing k into a two-peak shape with contributions from two lower-frequency excitations, which is reflected in Fig. 7. The low-frequency excitations in the

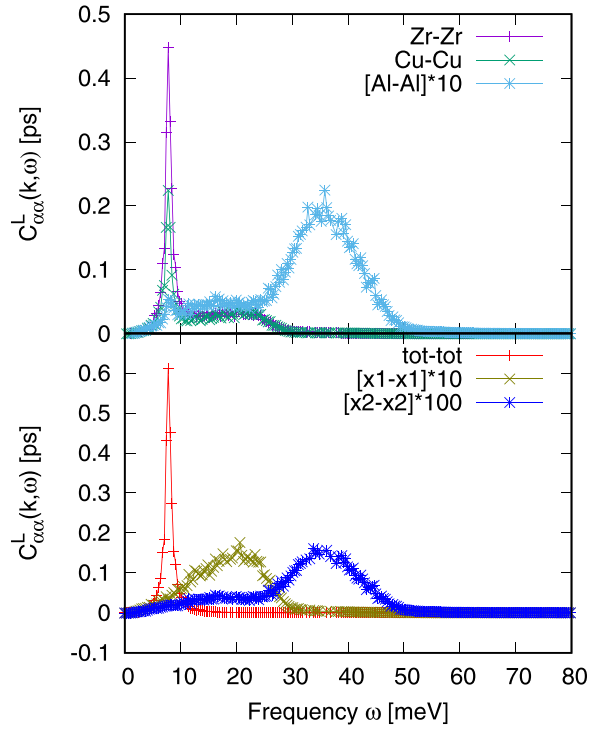


FIG. 6. Longitudinal current spectral functions corresponding to the mass-current autocorrelation functions at wave number $k = 0.1069 \text{ \AA}^{-1}$ shown in (top) Fig. 3 and (bottom) Fig. 4. The sharp low-frequency peak corresponding to acoustic excitations is present in all the partial spectral functions, while it is not present in long-wavelength spectral functions representing optic modes in the bottom panel.

long-wavelength region have almost linear dispersion laws with the speeds of L sound and T sound $c_L = 4329.9 \text{ m/s}$ and $c_T = 2148.5 \text{ m/s}$, respectively. One can see the L and T branches of two types of optic modes: The LO1 and TO1 branches in the long-wavelength region having the flat region $\sim 21\text{--}23 \text{ ps}^{-1}$ are due to the mutual motion of Zr and Cu atoms with opposite phases, and the LO2 and TO2 branches are due to the mutual motion of the light Al atoms in opposite phase to the motion of the heavy Zr and Cu atoms. Note that for $k > 2.5 \text{ \AA}^{-1}$ the frequencies of the three L and T branches are practically the same. Hence there is no reason to claim as in Ref. [35] that at $k \sim 3.8 \text{ \AA}^{-1}$, transverse excitations were detected in the scattering experiments.

Now we proceed with theoretical GCM analysis of transverse dynamics in the ternary ZrCuAl glass. The GCM theory for longitudinal dynamics in glasses [13] is based on subtraction of nonergodicity factors from the partial density-density time correlation functions and systematic accounting for the exact sum rules for the short-time behavior (frequency moments) and low-frequency behavior (time moments) of density-density correlations. Even for a two-component glass it is a sophisticated task of calculation of a 10×10 generalized k -dependent kinetic matrix $\mathbf{T}(k)$ and subsequent analysis of ten dynamic eigenmodes and their eigenvectors.

In order to rationalize the transverse dispersions and corresponding dampings of acoustic and nonacoustic collective modes shown in Fig. 7 via the observed peak positions

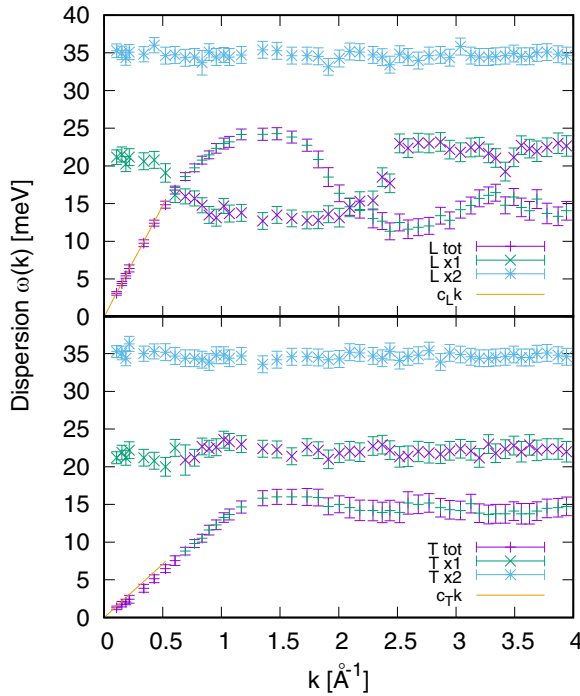


FIG. 7. Dispersion of longitudinal (top) and transverse (bottom) collective excitations, obtained from peak positions in the power spectra of autocorrelation functions $F_{\alpha}^{L/T}(k, t)$, $\alpha = \text{tot}, x1, x2$, Eqs. (2), (4), (5), and (6) (as shown in Fig. 6). For $k > 0.7 \text{ \AA}^{-1}$ the spectral functions contain more than one peak. The estimated speed of longitudinal sound is $c_L = 4329.9 \text{ m/s}$, and that of transverse sound is $c_T = 2148.5 \text{ m/s}$. The macroscopic linear dispersion laws are shown by the orange lines.

of $C_{\alpha}^T(k, \omega)$, $\alpha = \text{tot}, x1, x2$, we will apply more sophisticated extended dynamic models for transverse dynamics. It is known that the further extension of the viscoelastic (VE) model with “fast” dynamic variables generated via the higher (second and third) time derivatives of the transverse current, as was done in Refs. [29,45], leads to systematic improvement in the short-time behavior of the transverse current-current time correlation functions. However, this improvement in the short-time behavior does not allow one to improve the long-time behavior of $F_{JJ}^T(k, t)$ as well. Therefore a further direction for generalized hydrodynamic treatment is to improve the low-frequency behavior of current spectral functions by adding into the GCM scheme some “slow” dynamic variables which are statistically uncorrelated with the hydrodynamic ones [53]. This generalization was successfully applied in the study of low-frequency dynamics in a binary metallic glass [13] and for transverse dynamics in highly compressed liquid Li [51].

In our case, for the transverse dynamics in a three-component glass, one can extend the standard transverse VE model [25] by several slow dynamic variables in a manner similar to that followed in Ref. [51]. It appears that one can introduce a transverse analogy for the regular density-density time correlation functions, which can be a time correlation function constructed on the simplest slow extended transverse

dynamic variables

$$F_{II}^T(k, t) = \langle IJ^{T*}(k, 0)IJ^T(k, t) \rangle, \quad (9)$$

where the integral operator I [13] was defined as

$$IJ^T(k, t) = \int_{C_1}^t J^T(k, t') dt'$$

with C_1 being an arbitrary constant [53]. It is obvious that the time correlation function (9) is connected via the second time derivative to the standard transverse current autocorrelation function

$$-\frac{\partial^2}{\partial t^2} F_{II}^T(k, t) \equiv F_{JJ}^T(k, t),$$

and the time Fourier transform of $F_{II}^T(k, t)$ is rightly the transverse analogy of dynamic structure factor $S^T(k, \omega)$ suggested in Ref. [54].

We applied the extended viscoelastic scheme (EVE) with 12 ($N_v = 12$) dynamic variables

$$A^{(12T)}(k, t) = \sum_{\alpha=\text{tot}, x1, x2} \{I^2 J_{\alpha}^T(k, t), IJ_{\alpha}^T(k, t), J_{\alpha}^T(k, t), j_{\alpha}^T(k, t)\} \quad (10)$$

for calculations of the dynamic eigenmodes contributing to the shape of each partial or collective current-current time correlation function $F_{JJ}^T(k, t)$. The generalized hydrodynamic matrix $\mathbf{T}^{(12T)}(k)$ generated for the transverse 12-variable dynamic model (10) for the three-component glass was used in

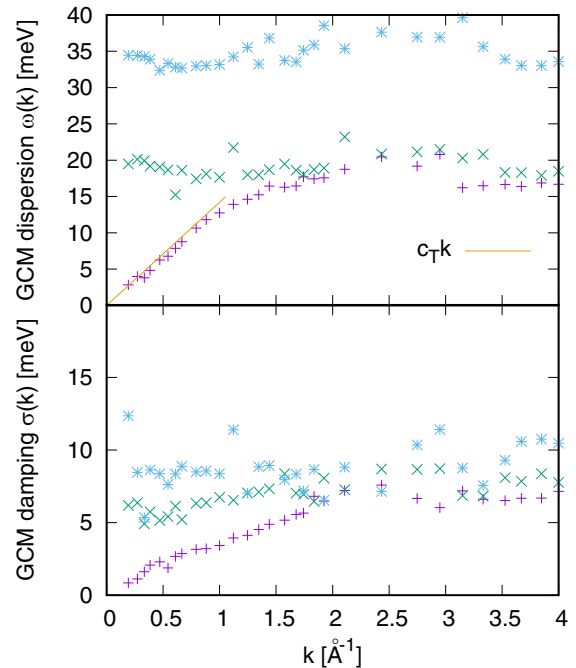


FIG. 8. Dispersion (imaginary parts of complex eigenmodes) and damping (real parts) of transverse dynamic eigenmodes, obtained from the extended GCM theory (10). The dispersion of the theoretical three branches of eigenmodes corresponds to the purely numerical dispersions obtained via peak positions of MD-derived current spectral functions in Fig. 7. The linear dispersion law with $c_T = 2148.5 \text{ m/s}$ is shown by the solid line.

the analysis of dynamic eigenvalues and eigenvectors contributing to the corresponding time correlation functions. In Fig. 8 we show the dispersion $\omega(k)$ and damping $\sigma(k)$ of theoretical transverse collective excitations, obtained from the GCM theory using the set (10). It is important that the GCM eigenvalues do not depend on the partial or total mass–mass-concentration representation of the dynamic variables in multi-component systems. Since the dynamic variables of the total mass–mass-concentration representation (2), (4), and (5) are linear combinations of the partial currents, the GCM eigenvalues will be exactly the same for all the sets of dynamic variables related by linear transformations. The theoretical GCM dispersions in Fig. 8 very well correspond to the dispersions of transverse excitations derived from peak positions of the transverse total and mass-concentration currents (Fig. 7), which is another support for the correctness of representation of collective dynamics in many-component disordered systems via acoustic and opticleike excitations. It is seen from the frequencies and damping of theoretical transverse eigenmodes (Fig. 8) that none of the collective modes has the damping with the sharp increase at the k_p that was proposed in Ref. [35]. Hence our theoretical dispersion curves and k -dependent damping of acoustic and nonacoustic collective modes do not show a damping proportional to $S(k)$ in the region close to k_p , the first sharp diffraction peak of $S(k)$.

IV. CONCLUSION

We conclude with the following results.

(i) We have shown the existence of nonacoustic collective modes in a three-component glass by suggesting several orthogonal linear combinations of partial currents, whose spectral functions in the long-wavelength region have a single-peak shape at distinct frequencies.

(ii) Our analysis for the metallic glass $\text{Zr}_{46}\text{Cu}_{46}\text{Al}_8$ shows the origin of the long-wavelength optic modes: LO1 and TO1 modes at $\omega \sim 21\text{--}23\text{ ps}^{-1}$ are due to the motion of Zr and Cu

atoms with opposite phases, and LO2 and TO2 modes are due to the motion of the light Al atoms with opposite phase to the motion of the Zr and Cu atoms.

(iii) The longitudinal and transverse optic modes are in the same frequency range. Moreover, for wave numbers $k > 2.5\text{ \AA}^{-1}$ the frequencies of all three branches of L and T modes practically coincide; hence, in Ref. [35], the signal from scattering experiments ascribed to the observation of a T mode is perhaps the signal from a nonacoustic L mode.

(iv) Our theoretical analysis of the frequencies and damping of acoustic and nonacoustic propagating modes within the extended viscoelastic model does not support the finding in Ref. [35] that the k -dependent damping of short-wavelength collective modes follows the shape of the total structure factor $S(k)$. None of our three propagating eigenmodes shows such specific k dependence of its damping. We hypothesize that the damping of the transverse mode observed in Ref. [35] is an artifact of the data analysis. Having neglected the existence of opticleike modes in the spectrum, the authors strongly overestimated the width of the TA modes, lumping together different excitations.

ACKNOWLEDGMENTS

T.B. was supported by National Research Foundation of Ukraine Grant No. 2020.02/0115. We acknowledge the CINES and IDRIS under Project No. INP2227/72914, as well as CIMENT/GRICAD for computational resources. This work was performed within the framework of the Centre of Excellence of Multifunctional Architected Materials CEMAM-ANR-10-LABX-44-01 funded by the “Investments for the Future” Program. This work has been partially supported by MIAI@Grenoble Alpes (ANR-19-P3IA-0003). Fruitful discussions within the French collaborative network and in artificial intelligence in materials science GDR CNRS 2123 (IAMAT) are also acknowledged.

-
- [1] W. Schirmacher, *Theory of Liquids and Other Disordered Media: A Short Introduction* (Springer, Berlin, 2014).
 - [2] J.-P. Hansen and I. R. McDonald, *Theory of Simple Liquids* (Academic, London, 1986).
 - [3] J.-P. Boon and S. Yip, *Molecular Hydrodynamics* (McGraw-Hill, New York, 1980).
 - [4] M. Baggioli, M. Landry, and A. Zaccone, *Phys. Rev. E* **105**, 024602 (2022).
 - [5] T. Bryk, W. Schirmacher, and G. Ruocco, *Phys. Rev. E* **106**, 036601 (2022).
 - [6] W. Schirmacher, G. Diezemann, and C. Ganter, *Phys. Rev. Lett.* **81**, 136 (1998).
 - [7] S. N. Taraskin and S. R. Elliott, *Phys. Rev. B* **61**, 12017 (2000).
 - [8] W. Schirmacher, G. Ruocco, and T. Scopigno, *Phys. Rev. Lett.* **98**, 025501 (2007).
 - [9] C. Caroli and A. Lemaitre, *J. Chem. Phys.* **153**, 144502 (2020).
 - [10] S. N. Taraskin and S. R. Elliott, *Europhys. Lett.* **39**, 37 (1997).
 - [11] S. N. Taraskin and S. R. Elliott, *Phys. Rev. B* **61**, 12031 (2000).
 - [12] J. Hafner, *J. Phys. C: Solid State Phys.* **16**, 5773 (1983).
 - [13] T. Bryk and I. Mryglod, *Phys. Rev. B* **82**, 174205 (2010).
 - [14] C. J. Benmore, S. Sweeney, R. A. Robinson, P. A. Egelstaff, and J. B. Suck, *J. Phys.: Condens. Matter* **11**, 7079 (1999).
 - [15] D. Crespo, P. Bruna, A. Valles, and E. Pineda, *Phys. Rev. B* **94**, 144205 (2016).
 - [16] S. Hosokawa, M. Inui, Y. Kajihara, T. Ichitsubo, K. Matsuda, H. Kato, A. Chiba, K. Kimura, K. Kamimura, S. Tsutsui, H. Uchiyama, and A. Q. R. Baron, *Mater. Sci. Forum* **879**, 767 (2017).
 - [17] T. Ichitsubo, S. Hosokawa, K. Matsuda, E. Matsubara, N. Nishiyama, S. Tsutsui, and A. Q. R. Baron, *Phys. Rev. B* **76**, 140201(R) (2007).
 - [18] T. Ichitsubo, E. Matsubara, K. Miyagi, W. Itaka, K. Tanaka, and S. Hosokawa, *Phys. Rev. B* **78**, 052202 (2008).
 - [19] T. Ichitsubo, W. Itaka, E. Matsubara, H. Kato, S. Biwa, S. Hosokawa, K. Matsuda, J. Saida, O. Haruyama, Y. Yokoyama, H. Uchiyama, and A. Q. R. Baron, *Phys. Rev. B* **81**, 172201 (2010).
 - [20] L. Pedesseau, S. Ispas, and W. Kob, *Phys. Rev. B* **91**, 134202 (2015).
 - [21] V. M. Giordano and B. Ruta, *Nat. Commun.* **7**, 10344 (2016).

- [22] B. Ruta, E. Pineda, and Z. Evenson, *J. Phys.: Condens. Matter* **29**, 503002 (2017).
- [23] X. Monnier, D. Cangialosi, B. Ruta, R. Busch, and I. Gallino, *Sci. Adv.* **6**, eaay1454 (2020).
- [24] S. Jahn and J.-B. Suck, *Phys. Rev. Lett.* **92**, 185507 (2004).
- [25] T. Bryk, *Eur. Phys. J.: Spec. Top.* **196**, 65 (2011); **227**, 2689 (2019).
- [26] S. Hosokawa, M. Inui, T. Bryk, I. Mryglod, W.-C. Pilgrim, Y. Kajihara, K. Matsuda, Y. Ohmasa, and S. Tsutsui, *Condens. Matter Phys.* **22**, 43602 (2019).
- [27] F. Demmel, S. Hosokawa, and W.-C. Pilgrim, *J. Phys.: Condens. Matter* **33**, 375103 (2021).
- [28] T. Bryk and I. Mryglod, *Phys. Lett. A* **261**, 349 (1999).
- [29] T. Bryk and I. Mryglod, *J. Phys.: Condens. Matter* **12**, 6063 (2000).
- [30] A. Jaiswal, T. Egami, and Y. Zhang, *Phys. Rev. B* **91**, 134204 (2015).
- [31] H. L. Peng, F. Yang, S. T. Liu, D. Holland-Moritz, T. Kordel, T. Hansen, and Th. Voigtmann, *Phys. Rev. B* **100**, 104202 (2019).
- [32] T. Bryk and I. Mryglod, *Condens. Matter Phys.* **10**, 481 (2007).
- [33] I. Pozdnyakova, L. Hennem, J.-F. Brun, D. Zanghi, S. Brassamin, V. Cristiglio, D. L. Price, F. Albergamo, A. Bytchkov, S. Jahn, and M.-L. Saboungi, *J. Chem. Phys.* **126**, 114505 (2007).
- [34] L. Hennem, I. Pozdnyakova, V. Cristiglio, S. Krishnan, A. Bytchkov, F. Albergamo, G. J. Cuello, J.-F. Brun, H. E. Fischer, D. Zanghi, S. Brassamin, M.-L. Saboungi, and D. L. Price, *J. Non-Cryst. Solids* **353**, 1705 (2007).
- [35] X. Y. Li, H. P. Zhang, S. Lan, D. L. Abernathy, T. Otomo, F. W. Wang, Y. Ren, M. Z. Li, and X.-L. Wang, *Phys. Rev. Lett.* **124**, 225902 (2020).
- [36] LAMMPS code, <http://lammps.sandia.gov/index.html>; S. J. Plimpton, *J. Comput. Phys.* **117**, 1 (1995).
- [37] Y. Q. Cheng, E. Ma, and H. W. Sheng, *Phys. Rev. Lett.* **102**, 245501 (2009).
- [38] Y. Q. Cheng and E. Ma, *Appl. Phys. Lett.* **93**, 051910 (2008).
- [39] N. Jakse, A. Nassour, and A. Pasturel, *Phys. Rev. B* **85**, 174201 (2012).
- [40] K. Lad, N. Jakse, and A. Pasturel, *J. Chem. Phys.* **136**, 104509 (2012).
- [41] T. Bryk and I. Mryglod, *J. Phys.: Condens. Matter* **14**, L445 (2002).
- [42] A. B. Bhatia, D. E. Thornton, and N. H. March, *Phys. Chem. Liq.* **4**, 97 (1974).
- [43] I. M. deSchepper, E. G. D. Cohen, C. Bruin, J. C. van Rijs, W. Montfrooij, and L. A. de Graaf, *Phys. Rev. A* **38**, 271 (1988).
- [44] I. M. Mryglod, I. P. Omelyan, and M. V. Tokarchuk, *Mol. Phys.* **84**, 235 (1995).
- [45] T. Bryk and I. Mryglod, *Phys. Rev. E* **63**, 051202 (2001).
- [46] R. A. MacPhail and D. Kivelson, *J. Chem. Phys.* **80**, 2102 (1984).
- [47] I. M. Mryglod and I. P. Omelyan, *Mol. Phys.* **90**, 91 (1997).
- [48] T. Bryk, A. Huerta, V. Hordiichuk, and A. Trokhymchuk, *J. Chem. Phys.* **147**, 064509 (2017).
- [49] T. Bryk, I. Mryglod, and G. Ruocco, *Philos. Mag.* **100**, 2568 (2020).
- [50] T. Bryk and I. Mryglod, *J. Phys.: Condens. Matter* **16**, L463 (2004).
- [51] T. Bryk, G. Ruocco, T. Scopigno, and A. P. Seitsonen, *J. Chem. Phys.* **143**, 104502 (2015).
- [52] H. Flores-Ruiz, M. Micoulaut, A. Piarristeguy, M.-V. Coulet, M. Johnson, G. J. Cuello, and A. Pradel, *Phys. Rev. B* **97**, 214207 (2018).
- [53] I. P. Omelyan and M. V. Tokarchuk, *J. Phys.: Condens. Matter* **12**, L505 (2000).
- [54] H. Shintani and H. Tanaka, *Nat. Mater.* **7**, 870 (2008).